Proto-neutron star structure within an extended lowest-order constrained variational method at finite temperature

S. Goudarzi and H. R. Moshfegh
Department of Physics, University of Tehran, Post Office Box 14395-547, Tehran, Iran
(Received 17 June 2015; published 10 September 2015)

The lowest-order constrained variational approach at finite temperature is extended by adding a semiphenomenological three-body force to its formulation. The equation of state (EOS) of hot asymmetric nuclear matter is obtained within the framework of the extended model. The density and temperature dependence of the mentioned three-body force is also discussed. The EOS of the proto-neutron star as well as its mass-radius relation is studied for several values of constant entropy and lepton fraction. We find that the maximum gravitational mass of the proto-neutron star is slightly sensitive to the value of the entropy and lepton fraction.

DOI: 10.1103/PhysRevC.92.035806 PACS number(s): 21.30.Fe, 21.65.Mn, 97.10.Cv, 97.10.Nf

I. INTRODUCTION

Studying the equation of state (EOS) of asymmetric nuclear matter at finite temperature plays a crucial role in understanding the dynamics of hot and dense nuclear systems, which are available in the laboratory through intermediate- and high-energy heavy-ion collisions and also in the astrophysical systems. Remarkable examples of such systems are supernova explosions and hot and lepton-rich neutron stars [proto-neutron stars (PNSs)], which are formed in the last stage of a type-II supernova collapse [1]. There are some significant differences between the characteristics of proto-neutron stars (0.5–1 s after core bounce) and those of cold neutron stars (some minutes after core bounce), which are caused by the effect of neutrino trapping. A high and almost constant lepton fraction ($Y_l = 0.3$–0.4) [2–4] and almost constant entropy per baryon ($S/A = 1$–2) [2–5], as well as the high temperature comparable to the Fermi energy of the composition, are among them. Therefore, in order to study the thermal evolution of a PNS, an equation of state at finite temperature is required.

The temperature dependence of the EOS of asymmetric nuclear matter has been investigated within various theoretical models such as the Brueckner-Hartree-Fock (BHF) approach [6,7], variational method [8], relativistic mean field theory (RMFT) [9–11], the theory of Green's functions [12], and the lowest-order constrained variational (LOCV) approach [13–15]. The structure of the proto-neutron stars has been also studied in the framework of some of the mentioned theoretical methods such as BHF [7,16] and RMFT [11,17,18]. A complete study of the structure of the neutron stars shortly after their birth is also presented by Prakash *et al.* [1] by applying various nuclear models. In the present work we intend to study the equilibrium structure of PNSs within the LOCV approach.

The LOCV model is a fully self-consistent one which was originally presented to calculate the properties of cold nuclear matter [19,20] by using Reid-type potentials [21,22]. Later on, this technique was generalized to finite temperature [13–15] and also to study the thermodynamic properties of various nuclear systems such as asymmetric nuclear matter [14,23], pure neutron matter (PNM) [24], and β-stable matter [25]. This model is also extended to include relativistic corrections at both zero [26] and finite temperature [27], and also is adapted to use more sophisticated potentials such as AV14 [28], AV18 [29], and UV14 [30] as the bare two-body interaction. One valuable feature of the LOCV method is that the energy of many-body systems can be calculated by considering the contribution of only first and second terms in the cluster expansion of the energy. This feature comes from the fact that the constraint imposed on this approach [31,32] keeps the value of the higher cluster terms small.

It is generally accepted that many-body approaches are unable to produce the correct empirical saturation properties of cold symmetric nuclear matter (SNM), i.e., $\rho_0 = 0.17 \pm 1$ fm^{-3} and $E_0/A = -16 \pm 1$ MeV (where ρ_0 is the baryon density and E_0/A denotes the energy per nucleon of the system at saturation point) in the case of using only two-nucleon interactions in the Hamiltonian. Therefore, three-body forces (TBF) are also required to avoid this deficiency. Beside that, the role played by the TBF in determining the properties of high-density nuclear systems is important and must be taken into account.

Motivated by the mentioned facts, one of the aims of the present work is to extend the finite-temperature LOCV approach by adding a three-body force to its procedure. To do this task, a semiphenomenological Urbana-type three-body force (UIX) [33,34] is used which has two adjustable parameters determined so that the saturation point of cold symmetric nuclear matter can be produced correctly.

In order to consider the TBF in the zero-temperature calculations, an effective two-body interaction is produced by averaging over the third particle coordinates and is added to the bare nucleon-nucleon potential. A detailed description of this procedure can be found in our previous work [35]. In the case of finite temperature, the effect of the TBF is included in the self-consistent LOCV procedure along a similar way. The AV18 potential is also used as the bare two-body interaction. The resulting EOS of hot asymmetric nuclear matter is then used as an input to investigate the equilibrium structure of the proto-neutron stars. The core of the PNS is supposed to be composed of an uncharged mixture of neutrons, protons, electrons, muons, and electron neutrinos as well as muon antineutrinos, which are in β equilibrium during the lifetime of the PNS. Three different values of entropy per baryon are

considered for determining the properties of the proto-neutron star. For the sake of comparison, calculations are done by using two different values for lepton fraction since different evolution calculations show different lepton numbers [2–4].

The article is organized as follows. In Sec. II we review briefly the LOCV many-body theory at finite temperature. The procedure of obtaining a temperature-dependent effective two-body force is also discussed in this section. Section III is devoted to the study of the hot and neutrino-trapped stellar matter at constant entropy. Results and discussion are presented in Sec. IV. Finally the conclusion is given in Sec. V.

II. THE LOCV FORMALISM AT FINITE TEMPERATURE

A brief review of extracting the EOS of hot asymmetric nuclear matter in the framework of the lowest-order constrained variational method is given in the following. The procedure of adding the TBF to the LOCV formalism at finite temperature is also discussed later in this section.

A. Asymmetric matter

The starting point of the calculations in the LOCV approach is to produce a trial wave function for many-body interacting systems at finite temperature T, which is defined as follows [15]:

$$\Psi_T(1\dots A) = F_T(1\dots A)\Phi^T(1\dots A), \tag{1}$$

where Φ^T represents the uncorrelated ground-state wave function of A independent nucleons at temperature T and F_T is an A-body correlation operator, which is usually written as the symmetrized product of two-body correlation function operators at finite temperature, i.e.,

$$F = \mathcal{S}\prod_{i>j} f_T(ij), \tag{2}$$

where $\mathcal{S}$ is the symmetrizing operator. $f_T(ij)$ is written as

$$f_T(ij) = \sum_{\alpha,p=1}^{3} f_\alpha^p(ij;T)O_\alpha^p(ij), \tag{3}$$

where $\alpha = \{J,L,S,T,T_z\}$ and $p = 2$, 3 for triplet channels with $J = L \pm 1$. Otherwise, p is set to unity. The operators $O_\alpha^p(ij)$ are written in the following form:

$$O_\alpha^{p=1-3} = 1, \left(\tfrac{2}{3} + \tfrac{1}{6}S_{12}\right), \left(\tfrac{1}{3} - \tfrac{1}{6}S_{12}\right), \tag{4}$$

where $S_{12} = 3(\sigma_1\cdot\hat{r})(\sigma_2\cdot\hat{r}) - \sigma_1\cdot\sigma_2$ is the usual tensor operator. The nuclear Hamiltonian can be written in the general form of

$$H = \sum_i \frac{p_i^2}{2m_i} + \sum_{i<j} V(ij), \tag{5}$$

where $V(ij)$ is a two-nucleon potential. The energy of the many-body system can be calculated by cluster expanding the expectation value of the nuclear Hamiltonian. In the LOCV method, one keeps only the first two terms of the cluster expansion series [36] and the small contribution of higher terms is neglected. Therefore, the energy functional is written as

$$E_B[f] = \frac{1}{A}\frac{\langle\Psi|H|\Psi\rangle}{\langle\Psi\mid\Psi\rangle} = E_1 + E_{MB} \cong E_1 + E_2, \tag{6}$$

where A is the total number of particles. The one-body term E_1 which is independent of $f_T(ij)$, is the Fermi-gas kinetic energy for asymmetrical nuclear matter,

$$E_1 = \sum_{i=n,p}\frac{\hbar^2}{2m_i\rho_B\pi^2}\int_0^\infty k^4 n_i(k)dk. \tag{7}$$

n and p labels indicate neutrons and protons, respectively, and $\rho_B = \rho_n + \rho_p$. ρ_i is the number density of each individual particle and is written as

$$\rho_i = \frac{N_i}{\Omega} = \frac{\nu}{2\pi^2}\int_0^\infty k^2 n_i(k)dk, \tag{8}$$

where ν stands for the degeneracy of the particle and $n_i(k)$ is the Fermi-Dirac distribution function, which is defined as the following (the Boltzmann constant K_B is set to unity):

$$n_i(k) = \frac{1}{\exp\{[\varepsilon_i(k) - \mu(\rho_i,T)]/T\}}, \tag{9}$$

with $\varepsilon_i(k) = \frac{\hbar^2k^2}{2m_i^*}$, where $m_i^*(\rho_i,T)$ is the effective mass and is considered as a variational parameter which minimizes the free energy of the system. $\mu(\rho_i,T)$ denotes the auxiliary chemical potential of particles and can be calculated by using the particle conservation relation, i.e., Eq. (8). We mention that the so-called true chemical potential is computed from the thermodynamic relation of $\mu_i = (\frac{\partial f}{\partial\rho_i})|_{T,V}$, where f is the free energy density.

The two-body energy in Eq. (6) is defined as

$$E_2 = \frac{1}{2A}\sum_{ij}\langle ij|W_T(12)|ij - ji\rangle, \tag{10}$$

with

$$W_T(12) = -\frac{\hbar^2}{2m}\left[f_T(12),\left[\nabla_{12}^2, f_T(12)\right]\right] + f_T(12)V(12)f_T(12). \tag{11}$$

This expression is now minimized with respect to the channel correlation functions but subject to the normalization constraint, which is considered as [15,37]

$$\frac{1}{A}\sum_{ij}\langle ij|f_p^2(12) - f_T^2(12)|ij - ji\rangle = 0, \tag{12}$$

where f_p is the modified Pauli function which has the following form:

$$f_p(r) = \left[1 - \frac{1}{\nu}\left(\frac{\gamma_i(r)}{\rho_B}\right)^2\right]^{-\frac{1}{2}}, \quad T_z = \pm 1, \\ = 1, \quad T_z = 0, \tag{13}$$

with

$$\gamma_i(r) = \frac{2\nu}{(2\pi)^2}\int_0^\infty n_i(k)J_0(kr)k^2dk, \tag{14}$$

where $J_L(x)$ is the spherical Bessel function of order L. The correlation functions are determined by solving the Euler-Lagrange differential equations which result from minimizing the two-body cluster energy. The reader is referred to the mentioned references for more detail.

The Helmholtz free energy per particle of baryons can now be extracted using the following relation:

$$F_B(\rho_B,X,T,m^*) = E_B(\rho_B,X,T,m^*) - TS_B(\rho_B,X,T,m^*), \tag{15}$$

where $X = \frac{\rho_n-\rho_p}{\rho_B}$ is the isospin asymmetry parameter and S_B denotes the entropy per particle of baryons, which is written as [38]

$$S_B(\rho_B,X,T,m^*) = -\frac{K_B}{\Omega\rho_B}\sum_{k,i}[(1-n_i(k))\ln(1-n_i(k)) + n_i(k)\ln(n_i(k))]. \tag{16}$$

At this stage Eq. (15) is minimized with respect to $m_i^*(\rho_i,T)$ and the resulting $F_B(\rho_B,X,T)$ is then used for determining various thermodynamic quantities of interest.

B. Three-body force

It is well known that the contribution of three-body forces in the energy of nuclear systems at supernormal densities is quite important and must be taken into account. On the other hand, these forces have a crucial role in reproducing the correct saturation point of cold symmetric nuclear matter. Motivated by these facts, in our previous work [35] the UIX [33,34] three-body force was adapted to the LOCV formalism at zero temperature. In the present work we intend to extend this procedure to finite temperature in a similar way as the zero-temperature case by producing an effective two-body potential. The general form of the semiphenomenological UIX interaction, which is a meson-exchange-based theory, is written as

$$V_{123} = V_{123}^{2\pi} + V_{123}^{R}, \tag{17}$$

where

$$V_{123}^{2\pi} = A\sum_{cyc}(\{X_{12},X_{23}\}\{\tau_1\cdot\tau_2,\tau_2\cdot\tau_3\} + \frac{1}{4}[X_{12},X_{23}][\tau_1\cdot\tau_2,\tau_2\cdot\tau_3]) \tag{18}$$

and

$$V_{123}^{R} = U\sum_{cyc}T(m_\pi r_{12})^2T(m_\pi r_{23})^2 \tag{19}$$

are the two-pion exchange contribution and the shorter-range phenomenological part, respectively [33]. The one-pion exchange operator X_{12} in Eq. (18) is defined as

$$X_{12} = Y(m_\pi r_{12})\sigma_1\cdot\sigma_2 + T(m_\pi r_{12})S_{12}. \tag{20}$$

Numerals 1, 2, and 3 indicate three different interacting nucleons with the Pauli spin and isospin of σ and τ, respectively. $Y(m_\pi r)$ and $T(m_\pi r)$ are the Yukawa and tensor functions. A and U are two adjustable parameters, which are determined in such a way that the EOS extracted from the LOCV method will be able to reproduce the correct saturation properties of symmetric nuclear matter at zero temperature.

In order to avoid the full three-body problem, a density-dependent effective two-body interaction at finite temperature, $\bar{V}_{12}(r,T)$, is produced by averaging over the third particle coordinates and is weighted by the LOCV two-body correlation functions at temperature T, i.e., $f_T(r)$, at each given baryon density ρ_B,

$$\bar{V}_{12}(r,T) = \rho_B\int d^3r_3\sum_{\sigma_3,\tau_3}f_T^2(r_{13})f_T^2(r_{23})V_{123}, \tag{21}$$

where V_{123} is given by Eq. (17). In order to use this interaction in the nuclear Hamiltonian, it is more convenient to rewrite Eq. (21) in an operator structure form. After doing some algebra, one can get the desired expression, which has the following form:

$$\bar{V}_{12}(r,T) = (\tau_1\cdot\tau_2)(\sigma_1\cdot\sigma_2)V_{\sigma\tau}^{2\pi}(r,T) + S_{12}(\hat{r})(\tau_1\cdot\tau_2)V_t^{2\pi}(r,T) + V_c^R(r,T), \tag{22}$$

with

$$V_{\sigma\tau}^{2\pi}(r,T) = \frac{2\pi}{r}\rho_B\int_0^\infty xdx\int_{|r-x|}^{|r+x|}ydyf_T^2(x)f_T^2(y) \times\sum_{cyc}\sum_{\sigma_3\tau_3}4A\times[Y(m_\pi x)Y(m_\pi y) + 2P_2(\cos\theta)T(m_\pi x)T(m_\pi y)], \tag{23a}$$

$$V_t^{2\pi}(r,T) = \frac{2\pi}{r}\rho_B\int_0^\infty xdx\int_{|r-x|}^{|r+x|}ydyf_T^2(x)f_T^2(y) \times\sum_{cyc}\sum_{\sigma_3\tau_3}4A\times[Y(m_\pi x)T(m_\pi y)P_2(\cos\theta_x) + T(m_\pi x)Y(m_\pi y)P_2(\cos\theta_y) + T(m_\pi x)T(m_\pi y)P], \tag{23b}$$

$$V_c^R(r,T) = \frac{2\pi}{r}\rho_B\int_0^\infty xdx\int_{|r-x|}^{|r+x|}ydyf_T^2(x)f_T^2(y) \times\sum_{cyc}\sum_{\sigma_3\tau_3}U\times[T(m_\pi x)T(m_\pi y)]^2, \tag{23c}$$

in the notation of Ref. [35]. Once these three components of the effective two-body interaction are determined for a given density and temperature, Eq. (22) can be added to the bare NN potential and calculations are performed in the way discussed earlier in this section.

III. COMPOSITION OF THE PROTO-NEUTRON STARS

In order to determine the properties of a PNS, an EOS of hot and dense stellar matter, which is a charge-neutral neutrino-trapped matter in β equilibrium, is required. In the absence of the hyperonic degrees of freedom, such matter is primarily composed of neutrons n, protons p, relativistic electrons e and muons μ, electron neutrinos ν_e, and muon antineutrinos $\bar{\nu}_\mu$. The charge-neutrality condition requires the

following equality:

$$q_p x_p + \sum_{l=e,\mu} q_l x_l = 0, \tag{24}$$

where $x_i = \frac{\rho_i}{\rho_B}$ is the relative population of particle i and q_i represents the electric charge. The β-equilibrium conditions explicitly read

$$\mu_n - \mu_p = \mu_e - \mu_{\nu_e} = \mu_\mu + \mu_{\bar{\nu}_\mu}, \tag{25}$$

where μ_i indicates the chemical potential of each particle. Because of the extremely small population of positrons and electron antineutrinos ($\frac{x_{e^+}}{x_{e^-}} < 10^{-6}$ and $\frac{x_{\bar{\nu}_e}}{x_{\nu_e}} < 10^{-5}$ [39]), the contributions of these particles are neglected in the present calculation. Since the core of the PNS is opaque with respect to neutrinos, the electron and muon lepton family number, which is defined as

$$Y_l = x_l - x_{\bar{l}} + x_{\nu_l} - x_{\bar{\nu}_l}, \tag{26}$$

must be conserved. The values of Y_e and Y_μ can be estimated by the gravitational collapse calculation of the white dwarfs at the onset of neutrino trapping. Such calculation has indicated that the following constraint on Y_e can be imposed [1]:

$$Y_e = x_e + x_{\nu_e} \approx 0.4. \tag{27}$$

Moreover, since no muons are present when neutrinos become trapped, the following relation must hold [1]:

$$Y_\mu = x_\mu - x_{\bar{\nu}_\mu} = 0. \tag{28}$$

Therefore, we fix the Y_l at those values. For the sake of comparison, the value of $Y_e = 0.3$ is also considered in the present work. The chemical potential of leptons and their neutrinos at a given temperature can be calculated by using Eqs. (8) and (9) with

$$\varepsilon_i(k) = \sqrt{(\hbar k_i c)^2 + m_i^2 c^4}, \quad i = e,\mu, \tag{29}$$

and

$$\varepsilon_i(k) = \hbar k_i c, \quad i = \nu_e,\nu_\mu, \tag{30}$$

where $\varepsilon_i(k)$ is the single-particle energy of the species i. Since the relation of $\mu_{\bar{\nu}} = -\mu_\nu$ is held between the chemical potential of particles and their antiparticles, the chemical potential of muon antineutrino can also be determined. By solving Eqs. (24) and (25) together with Eqs. (27) and (28) self-consistently at a given temperature and baryon density, the energy per baryon of each lepton is determined by using the general equation of

$$E_i^L = \frac{1}{\pi^2 \rho_B} \int_0^\infty \varepsilon_i(k) n_i(k) k^2 dk, \quad i = e,\mu,\nu_e,\bar{\nu}_\mu. \tag{31}$$

The entropy per baryon of leptons is also written as

$$S_L = -\frac{K_B}{\Omega \rho_B} \sum_{k,i} [(1 - n_i(k))\ln(1 - n_i(k)) + n_i(k)\ln(n_i(k))]. \tag{32}$$

Therefore, the Helmholtz free energy per baryon of leptons can be calculated by using the following equation:

$$F_L = \sum_i E_i^L - T S_L. \tag{33}$$

At this stage the free energy per baryon of the PNS matter denoted by F/A, which is defined as

$$F/A = F_B + F_L, \tag{34}$$

can be determined at a given temperature and baryon density.

In order to study the structure of the PNS, the isentropic description of hot stellar matter is required. Having the free energy per particle at a given density for several values of temperature, the entropy per baryon can be calculated from the following relation:

$$\frac{S}{A} = -\left(\frac{\partial F/A}{\partial T}\right)_{\rho_B}. \tag{35}$$

By inserting the above relation in the equation

$$\frac{E}{A}(\rho_B, X, S) = \frac{F}{A}(\rho_B, X, S) + \frac{S}{A} T(\rho_B, X), \tag{36}$$

one can calculate the total energy per baryon E/A of the system. The EOS is then given by the thermodynamic relation of

$$P = \rho_B^2 \left(\frac{\partial E/A}{\partial \rho_B}\right)_S. \tag{37}$$

Now by assuming the PNS as a spherically symmetric body of isotropic material which is in static gravitational equilibrium, its structure can be obtained from the hydrostatic equilibrium equations, namely the Tolman-Openheimer-Volkoff (TOV) equations [40] for the enclosed mass m and pressure P,

$$\frac{dP(r)}{dr} = -\frac{GM(r)\varepsilon(r)}{c^2 r^2}\left(1 + \frac{P(r)}{\varepsilon(r)}\right)\left(1 + \frac{4\pi r^3 P(r)}{M(r)c^2}\right) \times \left(1 - \frac{2GM(r)}{rc^2}\right)^{-1}, \tag{38}$$

$$\frac{dM(r)}{dr} = \frac{4\pi \varepsilon(r) r^2}{c^2}, \tag{39}$$

where $\varepsilon(r)$ is the total energy density and G denotes the gravitational constant. By numerically integrating Eqs. (38) and (39), the mass-radius relation of the PNS for a given central energy density can be obtained. In the next section we provide our results regarding the temperature dependence of the TBF as well as the structure of the PNS.

IV. RESULTS AND DISCUSSION

We first discuss the effect of increasing the temperature from zero to a finite one on the two-body correlation function $f_T(r)$ and the corresponding effective two-body interaction $\bar{V}_{12}(r,T)$. In the LOCV approach, two-body correlation functions can be extracted for each two-body channel. It is shown in our previous work [35] that the $^1S_0$ channel two-body correlation function has the most important contribution in calculating the effective two-body interaction. Therefore, all

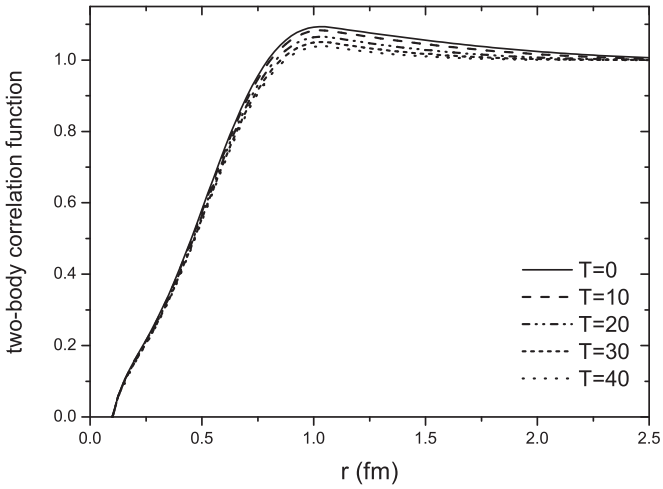

FIG. 1. The temperature dependence of $f_T(r)$ at $\rho_B = 0.17$ fm^{-3} for SNM.

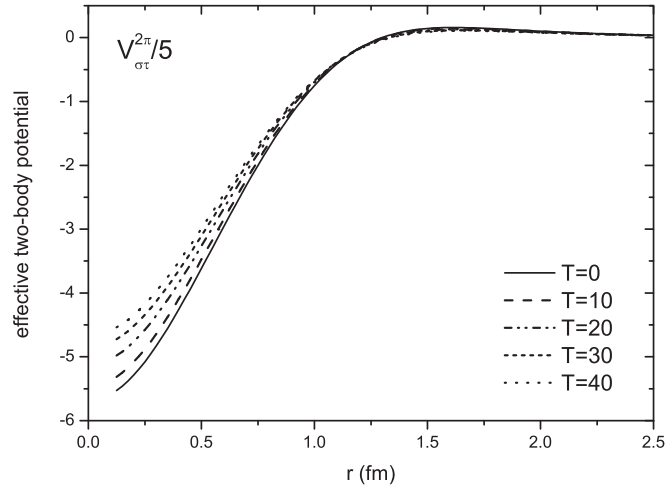

FIG. 3. The temperature dependence of the $V^{2\pi}_{\sigma\tau}$ component of the effective two-body interaction at $\rho_B = 0.17$ fm^{-3} for SNM.

of the following results are obtained by using the mentioned two-body correlation function in Eq. (21). The AV18 potential is also used as the bare two-body interaction. As is mentioned earlier, two parameters A and U of the UIX three-body force are adjusted in order to obtain a correct saturation point of cold SNM in the LOCV method. We use the values $A = -0.041$ MeV and $U = 0.000523$ MeV, yielding a saturation point at $\rho_0 = 0.1748$ fm^{-3} and $E_0 = -15.58$ MeV.

In order to study the temperature dependence of the two-body correlation function, $f_T(r)$ is plotted in Fig. 1 for several values of temperature at $\rho_B = 0.17$ fm^{-3} for SNM. As it expected, it is seen that at a fix relative distance between two particles, the correlation function is decreased by increasing the temperature.

The effect of increasing the baryon density at a fix temperature, namely $T = 10$ MeV, on $f_T(r)$ for symmetric nuclear matter is shown in Fig. 2(a). It is seen that $f_T(r)$ slightly decreases by increasing ρ_B, particularly after healing distance. There is no significant difference between the values of $f_T(r)$ at short distances and also after the effective potential range.

Figure 2(b) shows three components of the corresponding effective two-body potential, namely Eqs. (23a) to (23c). It can be seen that increasing the baryon density results in increasing the absolute value of all three components of the effective two-body potentials, as is expected, since the UIX three-body force is a density-dependent one. Therefore, one can predict that the repulsive effect of the TBF on the EOS will be stronger by increasing the baryon density.

The effect of increasing the temperature on different components of the effective two-body potential, i.e., $V^{2\pi}_{\sigma\tau}$, $V^{2\pi}_{t}$, and V^{R}_{c} for SNM at $\rho_B = 0.17$ fm^{-3} is shown in Figs. 3, 4, and 5, respectively, for several values of temperature between 0 to 40 MeV. It can be concluded from these figures that the absolute value of all components of $\bar{V}_{12}(r,T)$ decreases slightly with temperature, as is expected since the two-body correlation function which is used for obtaining $\bar{V}_{12}(r,T)$ shows the same behavior (see Fig. 1).

In Fig. 6 the density and temperature dependence of the Helmholtz free energy obtained following the procedure discussed in Sec. II is shown for both SNM [Fig. 6(a)]

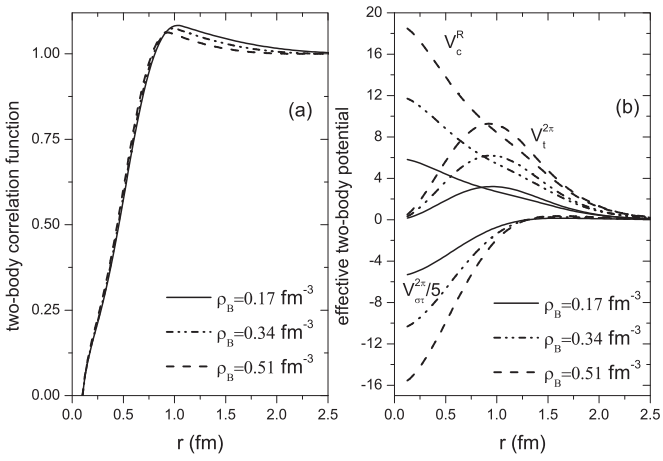

FIG. 2. (a) The density dependence of $f_T(r)$ at $T = 10$ MeV for SNM. (b) Same as panel (a) but for $\bar{V}_{12}(r,T)$.

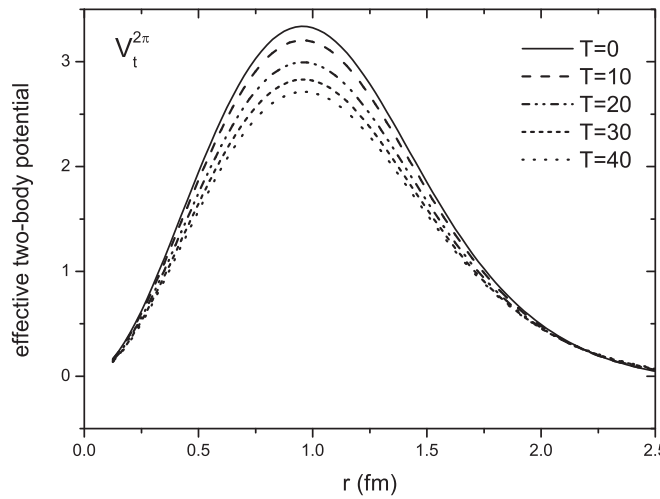

FIG. 4. Same as Fig. 3 but for the $V^{2\pi}_t$ component.

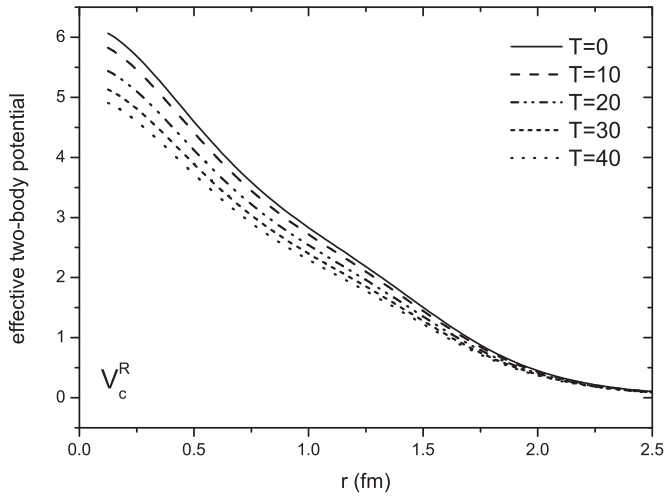

FIG. 5. Same as Fig. 3 but for the V_c^R component.

and PNM [Fig. 6(b)]. The effect of adding the TBF to the nuclear Hamiltonian on the free energy at different values of temperature is also shown in this figure. It is seen that because of the repulsive nature of the TBF, adding this force to the Hamiltonian makes the free energy of both SNM and PNM much stiffer at a given temperature compared to that obtained by using only AV18 potential and also shifts the saturation density toward lower densities in the case of SNM at zero temperature. Moreover, because of the density-dependent nature of the UIX three-body force, the repulsion from this interaction becomes stronger at each given temperature by increasing the baryon density, as is already concluded from Fig. 2(b). Mentioned results are in general agreement with those obtained within the BHF method [7].

As is mentioned in the text, in order to study the structure of the PNS, it is more convenient to switch from an isothermal to an isentropic description of hot and neutrino-trapped stellar matter. The starting point of obtaining the isentropic EOS of such matter is to find how the temperature changes as a

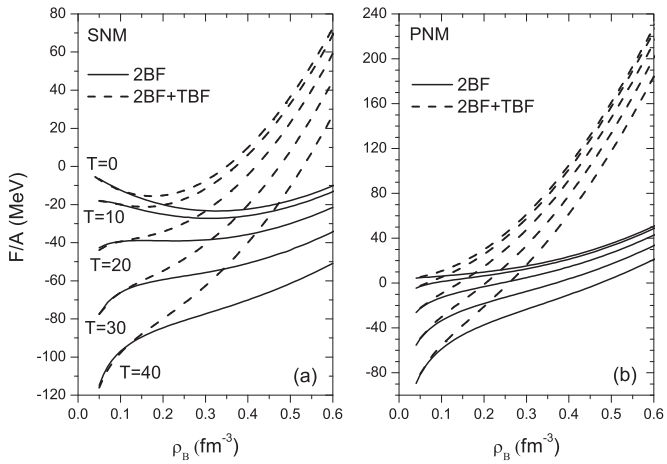

FIG. 6. (a) Free energy per baryon of the symmetric nuclear matter as a function of density for different values of temperature with and without the TBF. (b) Same as panel (a) but for the pure neutron matter.

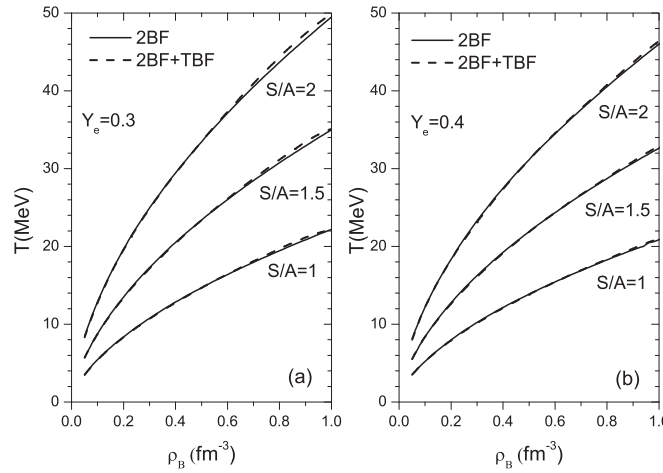

FIG. 7. (a) The temperature of the PNS matter as a function of baryon density for different values of entropy per baryon obtained with and without the TBF for $Y_e = 0.3$. (b) Same as panel (a) but for $Y_e = 0.4$.

function of baryon density ρ_B, as is shown in Fig. 7. For the sake of comparison, calculations are done for three different values of entropy per baryon, $S/A = 1,1.5,2$ MeV, and two values of lepton fraction, $Y_l = 0.3,0.4$ [Figs. 7(a) and 7(b), respectively], in both cases of using and not using the TBF. It is seen that in general the temperature is an increasing function of density. Moreover, higher values of temperature can be reached at systems which have larger values of the entropy. On the other hand, it is seen that the TBF dose not have a significant effect on the behavior of temperature as a function of density, particularly at the low-density region. However, the role of the TBF becomes clearer in a system with lower value of Y_e [Fig. 7(a)], since such system contains a larger number of neutrons and the TBF effects are stronger in such systems [see Fig. 6(b)]. By comparing Figs. 7(a) and 7(b) one can notice the effect of increasing the electron lepton family number Y_e on the relation between temperature and density of the PNS matter at a fixed entropy. It can be concluded that as the relative

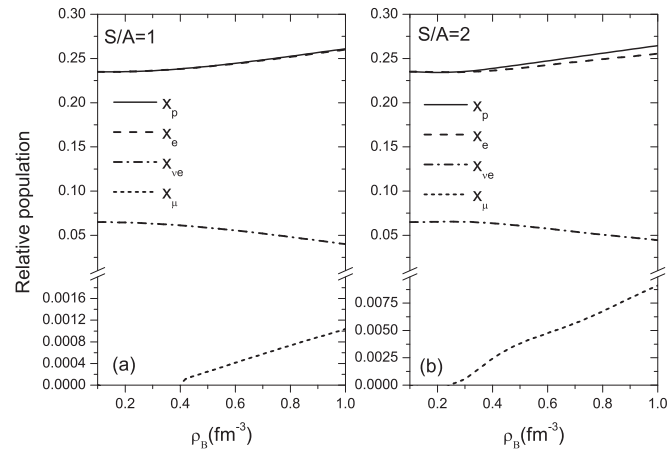

FIG. 8. (a) Relative population of the constituents of the PNS core calculated by using AV18 potential and for $Y_e = 0.3$ and $S/A = 1$. (b) Same as panel (a) but for $S/A = 2$.

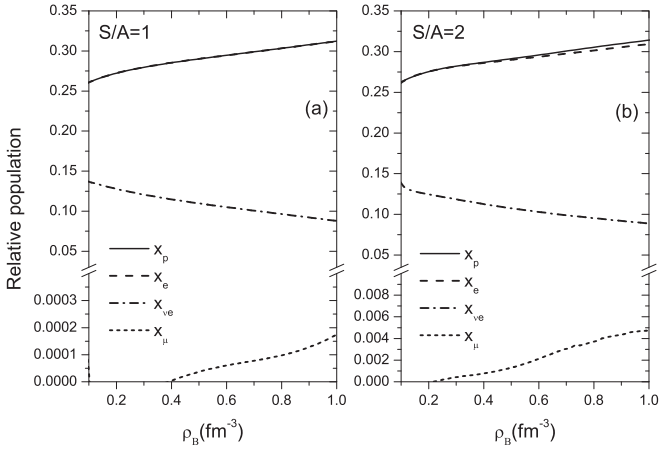

FIG. 9. (a) Relative population of the constituents of the PNS core calculated by using AV18 potential and for $Y_e = 0.4$ and $S/A = 1$. (b) Same as panel (a) but for $S/A = 2$.

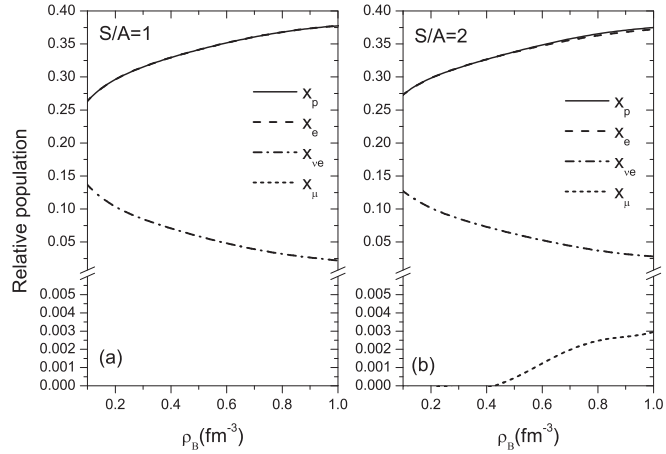

FIG. 11. Relative population of the constituents of the PNS core calculated by using AV18 + TBF potential and for $Y_e = 0.4$ and $S/A = 1$. (b) Same as panel (a) but for $S/A = 2$.

population of electrons and electron neutrinos increases, the temperature of the system decreases slightly at a given density for a fixed entropy.

Another important quantity regarding the hot and trapped stellar matter is the relative population x_i of the particles. In Figs. 8 to 11 the relative population of the constituents of the PNS matter is plotted as a function of baryon density for two values of S/A as well as two values of Y_e. The results obtained in the case of not using the TBF are plotted in Figs. 8 and 9. By comparing panels (a) and (b) of Figs. 8 and 9, It can be concluded that at a fixed Y_e, increasing the entropy mostly affects the relative population of muons, results in increasing the value of x_μ, and also makes the muons appear at lower densities. The same result is also reported in Ref. [16]. Moreover, it is seen that by increasing Y_e, the relative fraction of electron neutrinos increases correspondingly for all fixed entropies, as is expected. The same behavior can be seen in the case of using the TBF, i.e., Figs. 10 and 11. By comparing Figs. 8 and 9 with Figs. 10 and 11, one can conclude that at a fixed entropy and a fixed Y_e, using the TBF shifts the relative fraction of protons to larger values and correspondingly results in smaller values of x_{ν_e}. The TBF also makes the muons appear at lower densities compared to the case where the TBF is not used. We also remark the large value of proton fraction in the PNS which is in stark contrast to that of cold neutron stars. The value of this quantity turns out to be almost independent of entropy, particularly at high densities. An analysis of the cause of large value of x_p is given in Ref. [41].

In Figs. 12(a) and 12(b) the pressure of the PNS matter obtained from Eq. (37) is plotted against the baryon density for $Y_e = 0.3$ [Fig. 12(a)] and $Y_e = 0.4$ [Fig. 12(b)] at three fixed entropies and also for two cases of using and not using the TBF. It is seen that the EOS is not remarkably dependent on the entropy and the lepton fraction. In contrast, the TBF has a significant effect on the EOS of stellar matter because of its repulsive contribution to the free energy.

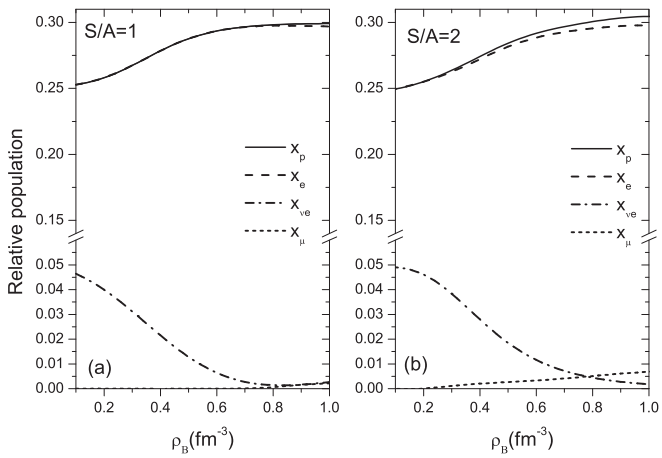

FIG. 10. Relative population of the constituents of the PNS core calculated by using AV18 + TBF potential and for $Y_e = 0.3$ and $S/A = 1$. (b) Same as panel (a) but for $S/A = 2$.

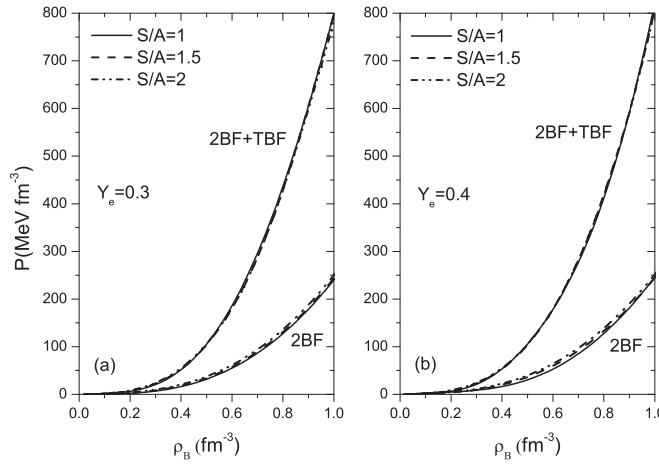

FIG. 12. (a) The EOS of the proto-neutron star with $Y_e = 0.3$ calculated with and without the TBF for some fixed values of the entropy per baryon. (b) Same as panel (a) but for $Y_e = 0.4$.

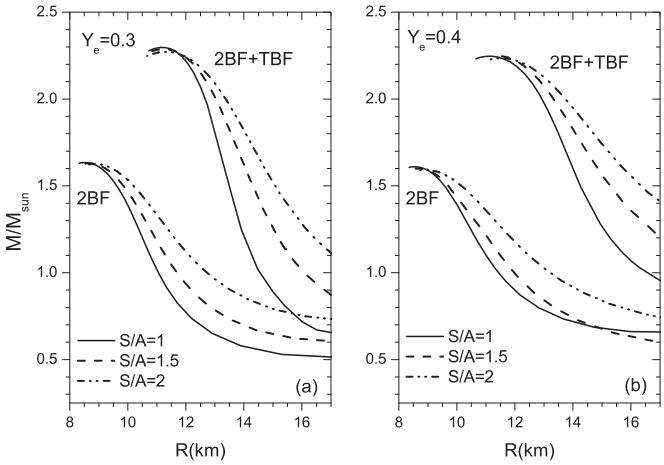

FIG. 13. (a) The mass-radius relation of the proto-neutron star with $Y_e = 0.3$ calculated with and without the TBF for some fixed values of the entropy per baryon. (b) Same as panel (a) but for $Y_e = 0.4$.

Let us now present our results regarding the PNS equilibrium structure. The core of the hot and neutrino-trapped PNS is described by the EOS presented above. A cold crust is also considered for the PNS by joining this EOS with the ones describe the medium- and low-density regimes obtained by Negele and Vautherin [42] ($0.001 < \rho < 0.08$ fm^{-3} and Baym *et al.* [43] ($\rho < 0.001$ fm^{-3}), respectively. By choosing an specific central energy density ε_c, the numerical integration of Eqs. (38) and (39) is done until the zero pressure is reached (the PNS surface). The resulting mass-radius relations for the PNS are plotted in Fig. 13 for cases of both using and not using the TBF and also for two different values of Y_e. The exact values of the maximum gravitational mass (in units of the solar mass) and the corresponding radii are reported in Table I together with those obtained within other methods for comparison. It can be concluded that for a fixed value of Y_e the maximum mass does not strongly depend on entropy, in contrast with the radius. However, since increasing the entropy results in increasing the number of protons of the system and correspondingly in softening the EOS, the value of the maximum mass slightly decreases with increasing the value of S/A. The same behavior is also seen in the results presented in Ref. [7], as is reported in Table I. On the other hand, as the value of Y_e increases the relative population of protons increases according to the charge neutrality condition (as can be seen in Figs. 10 and 11) and the EOS of baryonic part becomes softer. Therefore, a system with larger value of Y_e provides a smaller maximum mass compared to one with smaller value of Y_e with the same entropy. The effect of using the TBF on the mass-radius relation of the PNS is also shown in Fig.13. In general, as one can conclude from Fig. 12, the EOSs calculated by using the TBF produce larger gravitational masses compared to those obtained by using only two-body forces. More precisely, as can be seen in Figs. 13(a) and 13(b), calculations based on only two-body interaction result in maximum masses below 1.7 $M_\odot$, while the models containing TBF have maximum masses above $2M_\odot$, which is in agreement with the values that has been recently reported [44] for the mass of the neutron stars.

TABLE I. The maximum mass and the corresponding radius of the PNS obtained within the LOCV method as well as other approaches for some values of entropy and lepton fraction.

Method	Y_e	S/A	R (km)	$M/M_\odot$
LOCV(2BF)	0.3	1	8.5	1.63
LOCV(2BF)	0.3	1.5	8.6	1.63
LOCV(2BF)	0.3	2	8.8	1.62
LOCV(2BF)	0.4	1	8.5	1.61
LOCV(2BF)	0.4	1.5	8.6	1.60
LOCV(2BF)	0.4	2	8.9	1.59
LOCV(2BF + TBF)	0.3	1	11.1	2.29
LOCV(2BF + TBF)	0.3	1.5	11.2	2.29
LOCV(2BF + TBF)	0.3	2	11.2	2.27
LOCV(2BF + TBF)	0.4	1	11.1	2.24
BHF(2BF + TBF) [7]	0.4	1	10.2	1.95
LOCV(2BF + TBF)	0.4	1.5	11.3	2.24
LOCV(2BF + TBF)	0.4	2	11.5	2.23
BHF(2BF + TBF) [7]	0.4	2	10.7	1.95
Effective field theory [18]	0.4	2	13.2	1.76

V. CONCLUSION

The LOCV formalism at finite temperature is extended by introducing an effective two-body force. It turns out that the absolute value of the mentioned force decreases by temperature. By studying the relative population of the constituents of the hot neutrion-trapped stellar matter, we notice that the large values of proton fraction are available in the PNS. Those values of proton fraction are found to be almost independent of the entropy. It is also concluded that the onset of muons is strongly sensitive to the entropy and electron fraction as well as the TBF. In contrast, the maximum gravitational mass of the PNS turns out to depend weakly on the mentioned quantities. However, a slight decrease in the value of the maximum mass by increasing the entropy and electron fraction is observed. Finally, it is shown that the TBF is required in the Hamiltonian in order to theoretically predict a PNS with maximum masses above $2M_\odot$.

ACKNOWLEDGMENT

We thank the Research Council of University of Tehran for the grants.

[1] M. Prakash, I. Bombaci, M. Prakash, P. J. Ellis, J. M. Lattimer, and R. Knorren, Phys. Rep. **280**, 1 (1997); H. A. Bethe, Rev. Mod. Phys. **62**, 801 (1990); K. Strobel, C. Sohaab, and M. K. Weigel, Astron. Astrophys. **350**, 497 (1999); G. F. Marranghello, C. A. Z. Vasconcellos, and M. Dilling, Int. J. Mod. Phys. E **11**, 83 (2002).

[2] A. Burrows and J. M. Lattimer, Astrophys. J. **307**, 178 (1986).
[3] W. Keil and H.-Th. Janka, Astron. Astrophys. **296**, 145 (1995).
[4] J. A. Pons, S. Reddy, M. Prakash, J. M. Lattimer, and J. A. Miralles, Astrophys. J. **513**, 780 (1999).
[5] K. Sumiyoshi, H. Suzuki, and H. Toki, Astron. Astrophys. **303**, 475 (1995).
[6] W. Zuo, Z. H. Li, A. Li, and G. C. Lu, Phys. Rev. C **69**, 064001 (2004).
[7] M. Baldo and L. S. Ferreira, Phys. Rev. C **59**, 682 (1999); G. F. Burgio and H.-J. Schulze, Astron. Astrophys. **518**, A17 (2010).
[8] B. Friedman and V. R. Pandharipande, Nucl. Phys. A **361**, 502 (1981).
[9] J. D. Walecka, Ann. Phys. (NY) **83**, 491 (1974).
[10] N. K. Glendenning, Nucl. Phys. A **469**, 600 (1987); H. Muller and B. D. Serot, Phys. Rev. C **52**, 2072 (1995).
[11] G. Mahajan and S. K. Dhiman, Phys. Rev. C **84**, 045804 (2011).
[12] T. Frick, H. Muther, A. Rios, A. Polls, and A. Ramos, Phys. Rev. C **71**, 014313 (2005).
[13] H. R. Moshfegh and M. Modarres, Nucl. Phys. A **749**, 130 (2005).
[14] H. R. Moshfegh and M. Modarres, Nucl. Phys. A **792**, 201 (2007).
[15] H. R. Moshfegh and M. Modarres, Nucl. Phys. A **759**, 79 (2005).
[16] G. F. Burgio and H.-J. Schulze, Phys. At. Nucl. **72**, 1197 (2009).
[17] G. Shen, arXiv:1202.5791v1 [astro-ph.HE].
[18] I. Bednarek and R. Manka, Phys. Rev. C **73**, 045804 (2006).
[19] J. C. Owen, R. F. Bishop, and J. M. Irvine, Phys. Lett. B **59**, 1 (1975).
[20] M. Modarres and J. M. Irvine, J. Phys. G: Nucl. Phys. **5**, 511 (1979).
[21] R. V. Reid, Ann. Phys. (NY) **50**, 411 (1968).
[22] A. M. Green, J. A. Niskanen, and M. E. Sainio, J. Phys. G: Nucl. Part. Phys. **4**, 1055 (1978).
[23] M. Modarres, J. Phys. G: Nucl. Part. Phys. **19**, 1349 (1993).
[24] M. Modarres, J. Phys. G: Nucl. Part. Phys. **21**, 351 (1995).
[25] M. Modarres and H. R. Moshfegh, Phys. Rev. C **62**, 044308 (2000); Prog. Theor. Phys. **107**, 139 (2002).
[26] S. Zaryouni and H. R. Moshfegh, Eur. Phys. J. A **45**, 69 (2010).
[27] S. Zaryouni, M. Hassani, and H. R. Moshfegh, Phys. Rev. C **89**, 014332 (2014).
[28] R. B. Wiringa, R. A. Smith, and T. L. Ainsworth, Phys. Rev. C **29**, 1207 (1984).
[29] R. B. Wiringa, V. G. J. Stoks, and R. Schiavilla, Phys. Rev. C **51**, 38 (1995).
[30] I. E. Lagaris and V. R. Pandharipande, Nucl. Phys. A **359**, 331 (1981).
[31] M. Modarres, A. Rajabi, and H. R. Moshfegh, Phys. Rev. C **76**, 064311 (2007).
[32] M. Modarres, H. R. Moshfegh, and K. Fallahi, Eur. Phys. J. B **36**, 485 (2003).
[33] B. S. Pudliner, V. R. Pandharipande, J. Carlson, and R. B. Wiringa, Phys. Rev. Lett. **74**, 4396 (1995); B. S. Pudliner, V. R. Pandharipande, J. Carlson, S. C. Pieper, and R. B. Wiringa, Phys. Rev. C **56**, 1720 (1997).
[34] S. C. Pieper, V. R. Pandharipande, R. B. Wiringa, and J. Carlson, Phys. Rev. C **64**, 014001 (2001).
[35] S. Goudarzi and H. R. Moshfegh, Phys. Rev. C **91**, 054320 (2015).
[36] J. W. Clark, Prog. Part. Nucl. Phys. **2**, 89 (1979).
[37] G. H. Bordbar and M. Modarres, Phys. Rev. C **57**, 714 (1998).
[38] A. L. Fetter and J. D. Walecka, *Quantum Theory of Many-Body System* (McGraw-Hill, New York, 1971).
[39] T. Takatsuka, S. Nishizaki, and J. Hiura, Prog. Theor. Phys. **92**, 779 (1994).
[40] J. Oppenheimer and G. Volkoff, Phys. Rev. **55**, 374 (1939).
[41] T. Takatsuka, S. Nishizaki, and J. Hiura, Prog. Theor. Phys. **89**, 551 (1993).
[42] J. W. Negele and D. Vautherin, Nucl. Phys. A **207**, 298 (1973).
[43] G. Baym, C. Pethick, and D. Sutherland, Astrophys. J. **170**, 299 (1971).
[44] P. B. Demorest, T. Pennucci, S. M. Ransom, M. S. E. Roberts, and J. W. T. Hessels, Nature (London) **467**, 1081 (2010); J. Antoniadis *et al.*, Science **340**, 6131 (2013).